DOI: https://doi.org/10.14256/JCE.2125.2017

Građevinar 9/2018

Primljen / Received: 16.9.2017.
Ispravljen / Corrected: 4.4.2018.
Prihvaćen / Accepted: 11.4.2018.
Dostupno online / Available online: 10.9.2018.

Calculation procedure for determining wind action from vortex-induced vibration with verification of fatigue strength of steel structures

Authors:

Prof. Marina Rakočević, PhD. CE
University of Montenegro
Faculty of Civil Engineering
marinara@ac.me

Svetislav Popović, MSc. CE
Europoles GmbH & Co. KG
Neumarkt in der Oberpfalz, Deutschland
svelepopovic@gmail.com,
svetislav.popovic@europoles.com

Subject review

Marina Rakočević, Svetislav Popović

Calculation procedure for determining wind action from vortex-induced vibration with verification of fatigue strength of steel structures

An applicable calculation procedure, implemented with an object-oriented software that calculates amplitudes of oscillation due to vortex shedding, is presented in this paper using a stadium lighting pole as an example. The fatigue strength of material is proven, for the defined S-N curves, according to the nominal stress method. Available Eurocode-based calculation methods are also analysed and their advantages and disadvantages are presented.

Key words:
vortex shedding, fatigue of material, lock-in, spectral and resonant method, cantilever

Pregledni rad

Marina Rakočević, Svetislav Popović

Proračunski postupak za određivanje djelovanja vjetra pri vrtložnom osciliranju uz provjeru otpornosti na zamor čeličnih konstrukcija

U radu se na primjeru konzolnog nosača za osvjetljenje stadiona prikazuje primjenljiv proračunski postupak za koji je napisan objektno-orijentirani program koji izračunava amplitude osciliranja pri vrtložnom osciliranju. Za definirane S-N krivulje, dokaz pouzdanosti materijala na zamor se provodi prema metodi nominalnih naprezanja. Analiziraju se i dostupne metode proračuna iz Eurokoda i upućuje se na njihove prednosti i nedostatke.

Ključne riječi:
odvajanje vrtloga, zamor materijala, lock-in, spektralna i rezonantna metoda, konzola

Übersichtsarbeit

Marina Rakočević, Svetislav Popović

Berechnungsverfahren zur Bestimmung der Windeinwirkung bei wirbelerregten Querschwingungen mit Überprüfung der Betriebsfestigkeit von Stahlkonstruktionen

In der Abhandlung wird am Beispiel eines Kragarmträgers für die Stadionbeleuchtung das anwendbare Berechnungsverfahren dargestellt, für das ein objektorientiertes Programm geschrieben wurde, das die Amplitude der Schwingungen bei wirbelerregten Querschwingungen berechnet. Für die definierten S-N-Kurven wird der Nachweise der Betriebsfestigkeit des Stahls gemäß der Methode der Nennspannungen durchgeführt. Analysiert werden auch die zugänglichen Berechnungsmethoden aus dem Eurocode und es wird auf deren Vorteile und Nachteile hingewiesen.

Schlüsselwörter:
Wirbelerregung, Materialermüdung, Lock-in, Spektral- und Resonanzmethode, Kragarm

1. Introduction

The influence of the phenomenon of oscillation in transverse direction, in the case of free-standing cantilever structures subjected to vortex shedding, is a highly significant and topical issue for practicing engineers and scientific community. Slender structural girders such as chimneys, vertical lighting poles, overhead transmission lines, towers, and pylons, are particularly sensitive to this phenomenon, and must therefore be analysed with special care.

The starting assumption that the researchers of this phenomenon have agreed on is that the resonance problem in the lock-in state causes amplitudes which, although in most cases incapable of rapidly endangering bearing capacity of the structure on the global or local level, do constitute a hazard due to material fatigue effect, which is a direct consequence of the cyclic nature of the oscillation of structures in the resonant state. A usual graphical representation of von Karman's vortices for the mentioned oscillations is shown in Figure 1. Although there are many literature data on the limits of critical velocities causing resonant problems, an all-embracing model that could estimate with high level of certainty the effects of this phenomenon on the structures, at arbitrary flow regimens described by Reynolds number, has not as yet been proposed. That is why even today, decades after basic principles and values describing this phenomenon have been agreed upon, the theory is still being analysed and harmonized with the amplitudes and damage patterns observed in practical situations.

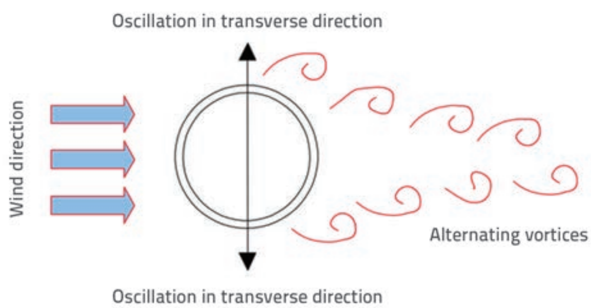

Figure 1. Von Karman's vortices

The experience has shown that in most cases the analysis of the above mentioned structures is directly dictated by proofs of fatigue of materials at individual critical details in which the concentration of stress occurs. This assertion gains a special importance in application of a simplified analysis that is based on the use of the nominal stress method. Thus it can often occur that, although the structure is not endangered by static action of external forces, a completely contrary conclusion can be made for the relevant design criterion – fatigue of material due to vortex shedding.

The proof of fatigue by means of more complicated local approaches that take into account the hot-spot or notch stress is an alternative that, in most cases from the everyday engineering practice, does not justify the time and resources invested, although such methods do lead to somewhat more favourable conclusions. However, reliability must strictly be proven for structures of special significances and this by conducting detailed theoretical, numerical, and experimental studies.

The best know models of vortex shedding applied in standards can be found in: Eurocode [1] Method 1 – harmonic/vortex-resonance method and Method 2 – spectral method, CICIND standards for steel chimneys – spectral method [2], Canadian standard NBC [3], Danish standard [4], and Australian/N. Zealand standard [5]. An unofficial "Hybrid Method" – ESDU (Item Nos. 96030 and 96031) [6, 7] is also often used in practice. Practical results obtained by this method have proven to be in good harmony with measured amplitudes of steel and concrete chimneys, cf. [8].

Regarding the last mentioned method, research has revealed that it estimates in a satisfactory way the oscillation amplitudes in the case of three out of four tested structures. That is why such calculation approach can be proposed as an alternative in case of large-size structures with high critical velocities when, at a low value of Scruton number, the vortex-resonance method can underestimate, and the spectral method can overestimate, the oscillation amplitude due to vortex shedding.

As already mentioned, two methods are used in Eurocode. The advantages and disadvantages of both methods are presented in available literature [8-21]. This literature enables us to derive conclusions about various assumptions and adequate consequences that may be expected if these calculation models are accepted as relevant. Theoretical bases for both calculation methods, with appropriate observations and suggestions, are presented in this paper.

The scope of this paper is limited to vortex shedding i.e. oscillation of the structure in transverse direction. It should be noted that oscillation parallel to the wind can also contribute to the total damage and can thus also be a subject of future research. In some specific structures, such as new generation of compact overhead transmission lines, the conductor galloping can significantly contribute to the total accumulation of damage, and so it must be taken into account in an appropriate way.

2. Theoretical bases

2.1. Spectral method

The spectral method, better known as Hansen method for calculation of vortex shedding, presented in EN 1991-1-4 [1], derives its roots from papers published by Vickery and Clark [22], which were additionally extended by Vickery and Basu [23-25]. According to Vickery-Basu Model, a general expression of the ratio of amplitude oscillation y_{max} on top of a uniform cantilever beam to critical section width b, in the first mode of oscillation, is written as follows:

$$\frac{y_{\max}}{b} = g\frac{\left[n_1 S_{cl}(n_1)\right]^{1/2}\left(\rho b^2 / m_e\right)}{16\pi^{3/2}\delta^{1/2}St^2}f(\phi) \qquad (1)$$

where:

g - maximum amplitude factor depending on resonance frequency (the value of this parameter varies between 3, 5 and 4)
n_1 - oscillation frequency in first mode
$S_{cl}(n)$ - spectral density of the coefficient of generalized transverse force
ρ - air density at vortex shedding
m_e - effective mass per unit length, given in F.4 [1]
δ - critical damping ratio containing structure damping and aerodynamic damping
S_t - Strouhal number, E.1.6.2 [1]
$f(\phi)$ - oscillation mode function.

It is presented in Eurocode [1] in the closed form for the first mode of oscillation as a spectral method for calculation of vortex shedding:

$$y_{\max} = \sigma_y k_{p};\left(\frac{\sigma_y}{b}\right)^2 = c_1 + \sqrt{c_1^2 + c_2};$$
$$c_1 = \frac{a_L^2}{2}\left(1 - \frac{Sc}{4\pi K_a}\right);\quad c_2 = \frac{\rho b^2}{m_e}\frac{a_L^2}{K_a}\frac{C_c^2}{St^4}\frac{b}{h} \tag{2}$$

where, in addition to the symbols already defined in Eq. (1):
k_p - peak factor
σ_y - standard deviation of displacement
S_c - Scruton number
C_c - aerodynamic constant, dependent on the cross-sectional shape, and for the circular cylinder also dependent on the Reynolds number Re, as defined in E.1.3.4, [1]; given in Table E.6, [1]
K_a - aerodynamic damping parameter, given in E.1.5.3 (4), [1]
α_L - normalised limiting amplitude giving the deflection of structures with very low damping, given in Table E.6 [1]
h, b - the height and width of structure; For structures with varying width, the width at the point with largest displacements is used.

By comparing measured amplitudes with the results of this model, Clobes, Willecke and Peil [10] observed that the model provides very rare and extreme values of oscillation amplitudes for low values of Scruton number, and that it is not suitable for application in the fatigue analysis of material in case of structures where a considerable safety is expected during service life (mostly 50 years). It is not suitable to combine the influence due to resonant oscillation according to this model with the number of loading cycles estimated according to expression (E.10) from [1], and this regardless of the bandwidth value adopted. The calibration of the total number of oscillations for use in combination with rare amplitudes calculated according to the spectral method has not as yet been presented in literature, and it greatly restricts the use of this method. Arbitrary setting this value to N > 200 · T leads to minimum number of oscillations amounting to 10^4, which is considered oversimplified and inadequate by the authors of this paper. In addition, assumptions from calculation models lead to the conclusion that this method has been excluded from the German national annex [26] for the following reasons: inconsistency of predicted results, use is limited to the basic mode of oscillation, use is limited to structures with regular distribution of dimensions along the main axis of the structure (which is in civil engineering practice typical for chimneys only), it cannot be used for elements in group or linear disposition, it cannot be applied for structures the response of which must be calculated using modal analysis and taking into account geometric nonlinearity of the system (i.e. for overhead transmission lines during their service life), and the model is highly dependent on local effects that influence the aerodynamic damping parameter. The authors consider that the spectral method – in its original form – without an appropriate extension of parameters of aerodynamic damping as a function of intensity of turbulence, as defined for instance in the French national annex [27], is in fact conservative and uneconomical. This type of spectral method would prevent construction of structures that are normally built in Central Europe, based on the current state-of-the-art. This assertion has also been confirmed by the author of the method [12].
As to laminar winds in case of temperature inversion, the authors' experience - based on construction of stadium lighting facilities in Norway - actually gives advantage to the spectral method, but not in the sense of material fatigue, but rather in the sense of taking into account large amplitudes in static sense, as they can be comparable to deflections of the structure caused by wind with the return period of 50 years. The spectral method will not be used in the calculation procedure given in the example. A more detailed analysis of this method, and the proposal for a practically applicable calculation procedure that would avoid at least some of the mentioned deficiencies, will be the subject of some future research.

2.2. Vortex - resonance method

The vortex-resonance method is based on the papers presented by Scruton et al. (summarized in [28]), Rumman [29], and Ruscheweyh [13-18, 30]. It is based on the assumption that the vortex shedding phenomenon creates sinusoidal forces of harmonic nature that are perpendicular to wind direction. Unlike spectral method, it is deterministic in nature and is based on a clearly defined mechanics.
The starting equation of the Ruscheweyh model is based on the modal force $Q(t)$ which is, for the normalised oscillation mode $\phi_{i,y}(z)$, described with:

$$Q(t) = \int_0^h F(z,t)\phi_{i,y}(z)dz \tag{3}$$

Symbols given in expression (3) are:
z - height coordinate of the girder of total height h;
$F(z,t)$ - cross-sectional wind load due to vortex shedding in time t, by unit length, where the following is valid

$$F(z,t) = q(z)b(z)c_F(z)\sin(2\pi n_{she}\cdot t + \gamma(z)\pi) \tag{4}$$

where:
$q(z)$ - dynamic velocity pressure
$b(z)$ - dimension (diameter or width) of cross section as a function of height coordinate
$c_F(z)$ - non-dimensional shape factor describing load amplitude
n_{she} - frequency of structure oscillation caused by vortices
$\gamma(z)$ - sign factor pointing to force orientation in the direction of the sign of mode shape.

It is assumed that these forces act at a particular length that is defined as "correlation length" L. The term itself comes from the field of stochastics, and its objective is to take aeroelastic effects into account. The space correlation coefficient R_{12} for fluctuating forces in two critical points along cross section is defined as:

$$R_{12} = \frac{\overline{f_1^{'}(t) f_2^{'}(t)}}{\overline{f^{'2}}} \tag{5}$$

where $f_1^{'}(t), f_2^{'}(t)$ are forces fluctuating along the unit length of a cylindrical body.
It is assumed that the mean quadratic fluctuating force $\overline{f^{'2}}$ is constant along the unit length, and so $\overline{f_1^{'2}} = \overline{f_2^{'2}} = \overline{f^{'2}}$.
For the cylinder cross section b, in case when the distance between two critical points is reduced, $R_{12}(\bar{r})$ where ($\bar{r} = r / b$) approaches 1. In the mentioned expression, $\bar{r}$ is the distance between two measuring points as a function of diameter b. When the defined critical points are spreading apart, $R_{12}(\bar{r})$ approaches zero. The expression (6):

$$\bar{L} = \int_0^{+\infty} R_{12}(\bar{r})\,d\bar{r} \tag{6}$$

where $\bar{L} = L / b$, defines the spatial limit of statistical events, such as small fluctuations of critical velocity, brief turbulent wind action, or synchronous vortex separation. In this way, the action of vortex forces (3) is limited to "correlation lengths" L that represent an empirical value based on measurements, and where $R_{12}(\bar{r})$ is mostly adopted in the form of an exponential function. A graphical presentation of spatial correlation of a cylindrical body is shown in Figure 2.

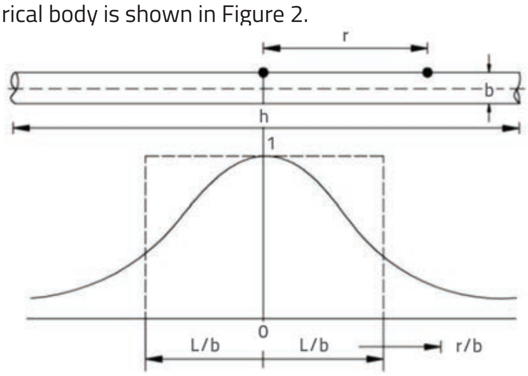

Figure 2. Spatial correlation of lateral forces for cylindrical body

A greater change in wind speed that disturbs the attained "synchronous state" is not included in this empirical parameter, and must be separately taken into account during estimation of the number of oscillations a structure is subjected to in the design-defined time period of construction and service life.
As it is already indicated that this is a resonance problem, the maximum response of the structure of height h is obtained in the case of "overlapping" or "matching" of the natural frequency $n_{i,y}$ of the ith oscillation mode with the frequency due to vortex action n_{she}, where the amplitude $y_{F,max}$ is realized for reference values of cross section b and the corresponding dynamic wind pressure:

$$\frac{y_{F,\max}}{b} = \phi_{i,y}(z)_{\max} \frac{\int_0^h \frac{q(z)}{q_{ref,b}} \frac{b(z)}{b} c_F(z) \phi_{i,y}(z)\,dz}{4\pi \int_0^h \phi_{i,y}^2(z)\,dz} \frac{1}{Sc} \frac{1}{St^2} \tag{7}$$

where the following symbols are used besides the already defined ones:
$\phi_{i,y}(z)$ - maximum normalised amplitude of oscillation
$q_{ref,b}$ - dynamic wind pressure at critical height with diameter b, where the vortex separation occurs.

Significance of Scruton number Sc and Strouhal number St was already recognized in initial models that described this phenomenon. The Scruton number describes the sensitivity of oscillations as a function of structural damping and the ratio of structural mass to fluid mass (air), by means of the following expression:

$$Sc = \frac{2\delta_s m_{i,e}}{\rho b^2} \tag{8}$$

where δ_s is the structural damping expressed by the logarithmic decrement, and $m_{i,e}$ is the equivalent mass per unit length for mode i, according to [1].
The damping of this model consists only of structural damping that is expressed in form of logarithmic decrement while, unlike spectral method, the aerodynamic damping is neglected. The reasons for this are manifold, and it is already indicated in theoretical bases of spectral method that the intensity of turbulence greatly influences the value of aerodynamic damping. This parameter is difficult to determine, which is why its estimation, in case of absence of appropriate guidance from standards, constitutes a highly challenging task for everyday engineering practice. The fundamental problem of detailed calculation in higher oscillation modes in the modal analysis of, for instance, an overhead transmission line at its operating stage, is related to the fact that the logarithmic decrement of damping defined in [1], Table F.2, provides guidelines for the fundamental oscillation mode only. In addition, the proposed values are not comprehensive, i.e. they provide guidelines for a particular type of structure only, so that in many cases

some additional assumptions have to be made. The analysis of measured amplitudes presented in [10] shows an exponential growth of oscillation amplitude for the values of $Sc < 5$. If the geometry of the structure is selected in such an unfavourable way, it is recommended to have special consultations with experts from the field of dynamic influences at wind load, so as to enable more appropriate interpretation of results. Strouhal number St describes the relationship between the critical wind velocity $V_{crit,i}$ and the natural frequency of the structure in the i-th oscillation mode $n_{i,y}$, with the following expression:

$$St = \frac{b \cdot n_{i,y}}{V_{crit,i}} \tag{9}$$

This expression provides an answer to the dependency of the critical wind velocity to the scalar value St and frequency characteristics of the structure. Many detailed data have been published about the St value in relevant literature. The proposal for adopting this value is presented in Figure 3. In most cases, this value is defined for circular cylinders as amounting to St ≈ 0.20. Experience shows that this conclusion is very often inadequate as the nature of vortex shedding is dependent on the flow regimen, which is defined by the Reynolds number. Thus the simplified value of 0.20 is mostly adopted for the subcritical area of flow regimen ($R_e < 2 \times 10^5$), while the St value mostly varies from 0.20 to 0.30 in the supercritical area ($R_e > 5 \times 10^6$). After introduction of EN 1991-1-4 this value was set to 0.18 for all values of the Reynolds number. Individual measurements have shown that this value may even amount to 0.16 for a low value of Reynolds number [10, 32]. That is why it is recommended in the calculation method to adopt the Strouhal number of 0.18 for all values of the Reynolds number, as defined in [1], while for structures of special significance it is recommended to conduct additional experimental and numerical investigations in order to make a more realistic estimation of this value.

In the sense of the so called maximum amplitude factor g that is also present in the spectral model (1), it can be stated that this factor is included in the Ruscheweyh resonance model through the following expressions:

$$\begin{aligned} \int_o^h c_F(z)\phi_{i,y}(z)dz &= gc_{lat}\int_{L^*}\phi_{i,y}(z)dz \\ gc_{lat}\int_{L^*}\phi_{i,y}(z)dz &= c_{lat}\int_{L_j}\phi_{i,y}(z)dz \end{aligned} \tag{10}$$

The meaning of expression (10) is not obvious and requires introduction of a new parameter called "effective correlation length" L_j and of the standard deviation of load in form of the value c_{lat} (round-mean-square value) that is defined in Eurocode as the "lateral force coefficient". In this way, the newly defined replacement effective correlation length contributes to the model by increasing the action of cross acting forces (4) by the factor of amplitude g which, in practice, varies from √2, that corresponds to harmonic excitation of the system described by vortex resonance model, and max. ≈ 4 that characterises the spectral model.

And, finally, by replacing equation (10) in (7) we obtain a recognisable form of equation for the amplitude of oscillation that is present in EN 1991-1-4, (E.7) [1]:

$$\frac{y_{F,max}}{b} = \frac{1}{St^2}\frac{1}{Sc}K \cdot K_w \cdot c_{lat} \tag{11}$$

In the equation (11), K stands for "mode shape factor". It is indicated in literature [30, 31] that the said parameter does not have a "physical significance". On the other hand, the effective correlation length factor K_w includes aeroelastic nature of forces through the phenomena described in equations (5), (6) and (10) in a simplified way, so that it is proportional to the set of dynamic pressure coefficients, when orthogonal solutions of the eigenvalue-problem of a cantilever beam are defined in the form of analogous functions. This assertion was used by Dickel who included all these observations in a developed calculation procedure [31, 34-36].

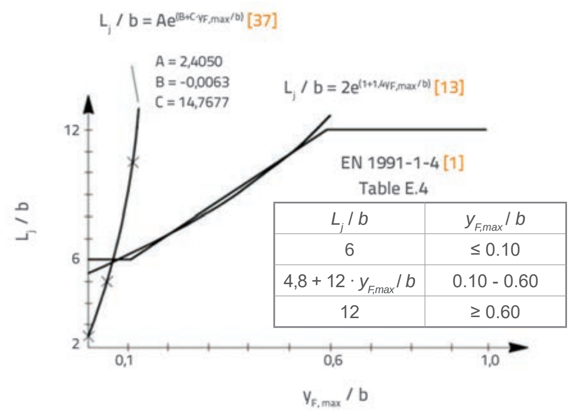

Figure 4. L_j/b as a function of dimensionless amplitude $y_{F,max}/b$, according to [1, 13, 37]

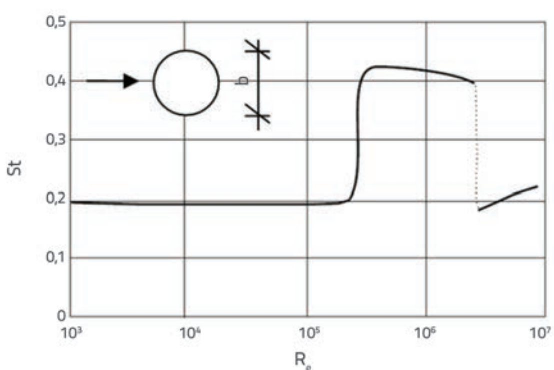

R_e	St
$10^5 \leq R_e \leq 4 \cdot 10^5$	0.19
$4 \cdot 10^5 \leq R_e \leq 10^6$	$-0.7674 + 0.1709 \log_{10}(R_e)$
$10^6 \leq R_e \leq 1.6 \cdot 10^6$	$1.3752 - 0.1862 \log_{10}(R_e)$
$R_e > 1.6 \cdot 10^6$	0.22

Figure 3. Strouhal number as a function of Reynolds number – left according to [8]; and right according to [33]

As the relationship between the dimensionless amplitude $y_{F,max}/b$ and the assumed effective correlation length L_j is the final criterion on convergence of the solution (Figure 4 according to [1, 13, 37]), it is necessary to use in the design an iterative procedure which, in case of high oscillation amplitudes, will not underestimate contribution of aeroelastic forces. The following final condition is proposed as the convergence criterion:

$$\varepsilon_{i,s} = \left| y_{F,max,i,s,k} / b_s - y_{F,max,i,s,k-1} / b_s \right| < 0{,}001 \tag{12}$$

The expression (12) emphasizes that the iterative procedure is conducted in all points of the girder (*s*) and, at that, the necessary number of iterative steps is marked with *k*. The procedure proceeds until fulfilment of the condition defined by expression (12), i.e. until attainment of the difference of less than 1‰ between two iterative steps.

By calculating the amplitude, the oscillation gains its quantitative meaning. Thus the amplitude of oscillation $y_{F,max,i,s}$ of an arbitrary point *s* in the oscillation mode *i* can be expressed as follows:

$$y_{F,max,i,s} = y_{F,max} \cdot \phi_{i,y}(s) \tag{13}$$

where $\phi_{i,y}(s)$ is the normalised value of the oscillation mode for the oscillation shape *i* in the point *s*.

As the final objective of the nominal stress calculation is to verify material fatigue, it is necessary to determine internal forces that occur along the girder length due to vortex shedding. The following expression is presented in Eurocode [1]:

$$F_w(s) = m(s) \cdot \left(2\pi n_{i,y}\right)^2 \phi_{i,y}(s)\, y_{F,max} \tag{14}$$

where $m(s)$ is the mass of the structure per unit length, while $F_w(s)$ are inertia forces per unit length of the girder. It can be noticed that this expression is only valid in case of a cylindrical structure where there are no discontinuities in mass and stiffness.

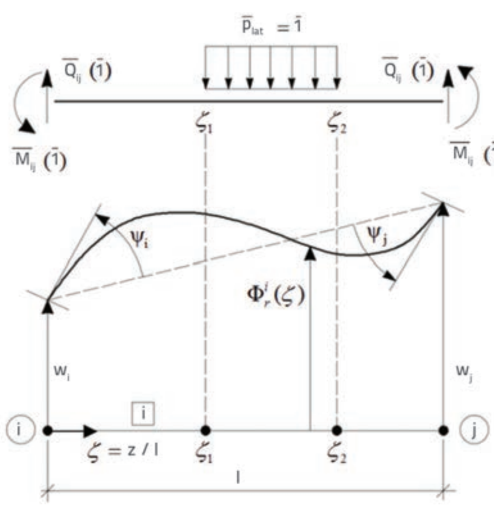

Figure 5. Generalized forces and displacements of the transversely loaded bar, according to [31]

This deficiency can very easily be avoided using the procedure presented in literature [31] that is based on the finite element method. For the bar finite element presented in Figure 5, starting from the normalised form of oscillation ϕ_r which satisfies the known form of eigenvalue problem:

$$[K]\phi_r - \omega_r^2 [M]\phi_r = 0 \tag{15}$$

the following solution X_r can be written for the oscillation mode *r* with circular frequency ω_r:

$$X_r = \phi_r e^{i\omega_r t} \tag{16}$$

The assumption of the defined force vector, as a function of the stiffness matrix *K*, mass matrix *M* and bar displacement vector v, is adopted as follows:

$$Q = [K] \cdot v + [M] \frac{\partial^2 v}{\partial t^2} \tag{17}$$

where: $Q^T = \left[Q_{ij}(t)\; M_{ij}(t)\; Q_{ji}(t)\; M_{ji}(t) \right]$ is the force vector, and $v^T = \left[w_i(t)\; \psi_i(t)\; w_j(t)\; \psi_j(t) \right]$ is the displacement vector, while stiffness matrix and mass matrix are derived for interpolation functions in form of Hermite polynomials for the bar exhibiting the length *l*, stiffness *EI* and weight per m' μ:

$$[K] = \frac{EI}{l^3} \begin{bmatrix} 12 & 6l & -12 & 6l \\ 6l & 4l^2 & -6l & 2l^2 \\ -12 & -6l & 12 & -6l \\ 6l & 2l^2 & -6l & 4l^2 \end{bmatrix} \quad [M] = \frac{\mu l}{420} \begin{bmatrix} 156 & 22l & 54 & -13l \\ 22l & 4l^2 & 13l & -3l^2 \\ 54 & 13l & 156 & -22l \\ -13l & -3l^2 & -22l & 4l^2 \end{bmatrix} \tag{18}$$

By applying expression (16), it can be concluded that $\ddot{v}_r = -\omega_r^2 v_r$ is valid which, once (17) is applied, leads toward local nodal forces of the element Q_r in the *r*-th form of oscillation mode, cf. [31]:

$$Q_r = y_{F,max} \left[[K] - \omega_r^2 [M] \right] \phi_r^{ij} \tag{19}$$

For tapered elements, i.e. for element with an inclined sides, it is possible to obtain a mean value of the moment of area at ends, with discretisation to small elements, which has in fact been applied in the calculation procedure defined in this paper, in such a way that $\bar{I}_{ij} = 1/\left(\left(1/2I_i\right) + \left(1/2I_j\right)\right)$, while the replacement value for μl in the mass matrix is adopted as the difference of normal force at bar ends, according to the theory of first order, taking into account contribution of concentrated masses.

3. Calculation procedure

3.1. Calculation of actions due to vortex shedding

All theoretical observations presented in Section 2.2 have been implemented in the authors' own object oriented software package that offers solution to quantitative oscillation due to vortex shedding, as well as appropriate internal forces that can be used to calculate nominal stresses. The software can also be used for calculation of hybrid structures created by combining several materials such as concrete, steel, or glass fibre reinforced polymers (GFRP).

The authors' own program for determining influences due to vortex shedding was written in the object-oriented code because of complexity of the calculation procedure. Specialized classes were derived using the inheritance method, which is particularly favourable in repeated use, namely in the iterative calculation procedure for calculating amplitude as a function of an assumed effective correlation length.

The evolution of expression (19) can be made using modal analysis, which was implemented in the calculation procedure via the link with an external program (COM technology). The COM (Component Object Model) is an industrial binary-interface that enables inter-process communication of objects in a wide variety of programming languages. In the scope of program development, it was used to link its own program based on object-oriented code written in C++ programming language, with the external program "RFEM-/RSTAB-Zusatzmodul RF-COM/RS-COM" [38]. This program extension offers two possibilities and both of them are based on modal analysis.

To begin with, it is possible to make an additional evaluation of the solution calculated using expression (13). The objective of the numerical procedure is to define the system's response in the sense of displacement of points according to expressions (11) and (13) and this for the assumed harmonic forces that are proportional to the product of nodal masses $m(s)$ and the corresponding displacements of each point of the selected oscillation mode:

$$F_w(s) = \pm m(s)\cdot \phi_{i,y}(s)\, y_{F,\max} \sin\left(2\pi n_{i,y}\cdot t\right) \tag{20}$$

These forces act on synthetic correlation lengths L_{sj} that are equal to the distances between zero points of the normalised oscillation mode. This model requires adoption of the corresponding damping model. The authors of this paper suggest application of the Rayleighs' proportional damping.

The differential equation of motion of the system under external load $F(t)$ that is variable in time can be expressed as follows:

$$\left[M\right]\left\{\ddot{y}(x)\right\} + \left[C\right]\left\{\dot{y}(x)\right\} + \left[K\right]\left\{y(x)\right\} = \left\{F(t)\right\} \tag{21}$$

where $y(x)$ are displacements of points, $\dot{y}(x)$ is the velocity, and $\ddot{y}(x)$ is the acceleration.

This traditional equation defines the system in which external forces are given as a function of the matrix of mass $[M]$, damping $[C]$ and stiffness $[K]$ of the system. Viscous damping is expressed as the combination of mass and stiffness, as follows:

$$\left[C\right] = \alpha\left[M\right] + \beta\left[K\right] \tag{22}$$

Coefficients α and β will be determined according to the following calculation procedure. Structural damping is adopted for the frequency corresponding to the basic mode in the amount as defined in [1] by converting the logarithmic decrement δ_s into relative damping ζ. The fixed value ζ amounting to 0.05 is defined for the oscillation mode m that is associated with the frequency at which a considerable percentage of mass participation, greater than 90 %, is realised. Therefore we have (23):

$$\omega_d = \omega\sqrt{1-\varsigma^2} \approx \omega \tag{23}$$

where ω_d is the circular frequency of the damped system, and ω is the circular frequency of the undamped system. However, due to small damping value, expression (20) can be considered in the same form for both damped and undamped system.

Damping values in modes that are situated in the range between the base mode and mode m are calculated by means of linear interpolation (24):

$$\varsigma_i = \frac{\varsigma_m - \varsigma_1}{\omega_m - \omega_1}(\omega_i - \omega_1) + \varsigma_1 \tag{24}$$

As simple linear interpolation is often insufficient, and as it potentially does not take into account possible nonlinear reduction in damping value at lower frequencies due to small contribution of stiffness matrix to the total damping, it is necessary to extend the set of data by extrapolation of results until 2.5 m modes of oscillation. For the frequency range above the mode m, the extrapolation can be made using the following expression (25):

$$\varsigma_i = \frac{\varsigma_m - \varsigma_1}{\omega_m - \omega_1}(\omega_{m+i} - \omega_m) + \varsigma_m \tag{25}$$

Finally, by solving the expression (26):

$$\begin{aligned} \beta_1 &= \frac{2\varsigma_1\omega_1 - 2\varsigma_m\omega_m}{\omega_1^2 - \omega_m^2} \qquad \alpha_1 = 2\varsigma_1\omega_1 - \beta_1\omega_1^2 \\ \beta_{2,5m} &= \frac{2\varsigma_1\omega_1 - 2\varsigma_{2,5m}\omega_{2,5m}}{\omega_1^2 - \omega_{2,5m}^2} \qquad \alpha_{2,5m} = 2\varsigma_1\omega_1 - \beta_{2,5m}\omega_{2,5m}^2 \end{aligned} \tag{26}$$

the damping of the system becomes fully defined for each data set. Indices 1, i.e. 2.5 m in expressions for α and β point to the set of data from which coefficients are calculated. A new data set is obtained by averaging the results obtained for the sets $(\varsigma_1, \varsigma_m, \omega_1, \omega_m)$ and $(\varsigma_1, \varsigma_{2,5m}, \omega_1, \omega_{2,5m})$. Graphical representation of relative damping as a function of circular frequency for various oscillation modes enables observation of the set that has the greatest reduction in damping value at lower modes. Coefficients α and β are defined for such set using expression (26).

The calculation using time integration in frequency domain is iterative in character and is repeated until a desired harmonic response is attained. The time step Δt and the final value of applied damping have the greatest influence on the shape of response of the system. Decrease of time step often positively influences attainment of a stable, harmonic response of the system.

An unstable and stochastic response can be noted for very low damped structures, especially for a girder composed of mixed materials. In this case, the adequacy of this model can become questionable. In the engineering practice, the procedure in which damping is increased by appropriate coefficients is in most cases sufficiently accurate for preliminary calculations. Calculated internal forces are also multiplied by the same coefficient. As simple multiplication of coefficients α and β can lead to results that are not on the side of safety, the authors suggest the use of the Lehrsch-relative damping for preliminary assessments in such non-standard cases. The proposed coefficient of multiplication of damping and the calculated internal forces amounts to 10. This value should be taken as an approximation only, and it is up to the practising engineer performing the calculation to carefully select the factor by which the damping and internal forces should be multiplied. The use of the proposed coefficient has been proven appropriate on a large number of preliminary estimations and feasibility studies in Germany, in the case of concrete telecommunication poles. Vertical extension of these poles was planned by adding steel or polymer reinforced glass fibres or antenna on top of the structure. The use of this principle enables reduction of inconsistencies to a reasonable level. This approach is not adequate for detailed analyses or final calculations as it may lead to disproportionality in response of the system and adopted damping.

The advantage of this calculation approach lies in the information about the time in which the structure will attain its resonance maximum. If this time is too short, i.e. if it is established by integration of the differential equation of motion (21) that the amplitude is attained several seconds after force application, especially within the first two oscillation modes, then this points to the low damping of the system and to great susceptibility to the vortex shedding phenomenon.

The use of this advantage, in combination with appropriate interpretation of Scruton number, which should not amount to less than 6, has proven to be a good engineering practice as evidenced by examples of several hundreds of steel, concrete and hybrid girders that have been designed and built by users of the program that is based on the mentioned calculation procedure.

Another advantage offered by modal analysis is related to limiting and geometrical conditions that have not been covered in an obvious way by assumptions of the vortex-resonance model, according to algorithm shown in Figure 6. Thus, for a tapered structure, it can not be stated with certainty that the position of "antinodes" with the maximum value of normalised oscillation mode represents the position of critical cross-section for the vortex separation, considering the change in the diameter or the width in points close to the critical one.

Vickery and Clark [22] showed that, in case of these structures, there is a great probability of occurrence of critical cross-section b at the height z in oscillation mode j, with the validity of a following expression (27):

$$\frac{d\left[b^4(z)\phi_j(z)\right]}{dz}=0 \tag{27}$$

For the situation of initial vortex separation in the zone close to the top of the structure, it can be expected that the increase in wind velocity could potentially "descend" the vortices towards lower cross-sections, which is a direct consequence of the variability of structural geometry. It is clear that in the case of tapered structures the spatial coefficient of correlation increases, and the aerodynamic contribution of forces decreases, but, at the first glance, it remains unclear in what way this would affect the entire response of the system, considering disproportionality of the change of these values. Due to these unknowns that require further research of this phenomenon, the authors of this paper recommend, based on practical experience, that special consultations with experts from this field be made in case of structures with taper greater than 25 mm/m. It is not unusual that these unknowns be taken into account in such cases by increasing the effective correlation length. This can be done using modal analysis in the frequency area according to the right branch of the algorithm presented in Figure 6. Harmonic forces acting on the structure in j effective correlation lengths L_j with critical cross-sections b_j can be written as follows:

$$\begin{aligned} F_{i,j} &= \pm F_{i,j,0}\sin(2\pi n_{i,y}\cdot t)\\ F_{i,j,0} &= \frac{1}{2}\rho v_{crit}^2 c_{lat} b_j L_j \end{aligned} \tag{28}$$

where the index i denotes the oscillation mode under consideration.

Table 1. Comparison with reference structure (b = 914 mm)

$n_{i,y}$ [Hz]	δ	c_{lat}	St	v_{crit} [m/s]	M [t/m]	K	Sc	K_w	$y_{F,max}$ [mm]	Source
1.721	0.015	0.241	0.20	7.87	0.090	0.129	2.59	0.465	128	This investigation
1.720	0.012	0.250	0.21	7.50	0.090	0.133	2.10	0.560	183	[16]
1.700	0.012	0.200	0.20	7.80	-	0.130	2.10	0.525	149	[39]
2.017	0.015	0.200	0.20	9.22	0.075	0.128	2.16	0.488	132	[35]
1.721	0.012	0.287	0.21	7.49	0.090	0.128	2.07	0.521	192	[35]
1.721	0.012	0.250	0.21	7.49	0.090	0.128	2.07	0.496	159	[35]
1.721	0.015	0.242	0.20	7.86	0.090	0.128	2.59	0.474	130	[35]
1.721	0.015	0.200	0.20	7.86	0.090	0.128	2.59	0.452	103	[35]

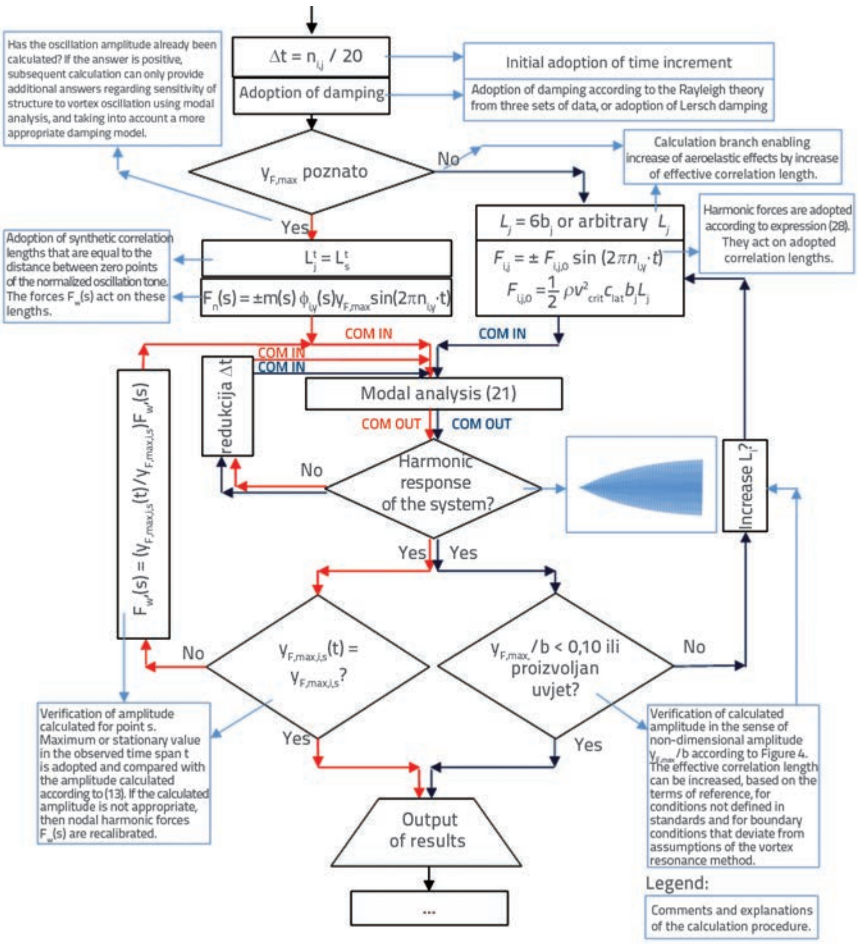

Figure 6. Calculation algorithm for modal analysis in resonant area using Component Object Model (COM) technology

In order to evaluate the calculation model presented in this paper, a comparison was made with the reference structure that has often been analysed in literature: steel chimney in Aachen, Germany. The comparison of results is presented in tabular form, as shown in Table 1. A good correspondence of results can be noted for oscillations in the natural mode, with a slight deviation from the measured amplitude. The oscillation amplitude of 140 mm was measured at the frequently observed frequency of 1.72 Hz [16, 31]. The results are related to the assumption of fixed support at the bottom of the structure, which is why they deviate from individual results that are based on the assumption of elastic support, c_D = 5.85·10^5 [kNm/m]. The calculated deviation of 8.6% from the measured amplitude can be explained by simplifications in the calculation, and by imperfections of the calculation model.

3.2. Fatigue analysis

From the above presented theory, it is clear that a structure can oscillate at various frequencies and, additionally, the vortex separation can occur at various heights in the same frequency mode. This leads toward various oscillation amplitudes, i.e. various states of stress during the defined service life of the structure. Thus, during their construction and use, structures are subjected to a spectrum of harmonic forces, for which structural resistance to material fatigue has to be proven. Eurocode [40] offers two possibilities in this respect.

The first calculation procedure is based on the known Palmgren-Miner rule. The same rule is applied in EN 1993-1-9 [40], and can be written as follows:

$$D = \sum_i \left[\frac{n_i(\Delta\sigma)}{N_i(\Delta\sigma)} \right] \tag{29}$$

where $n_i(\Delta\sigma)$ is the number of cycles of stress load for a specified stress range $\Delta\sigma = \sigma_{max} - \sigma_{min}$, for which $N_i(\Delta\sigma)$ cycles of load is expected before the structure suffers damage. D stands for total damage.

For the selected connection detail, the resistance to fatigue is defined by the material fatigue curve (S-N curve), Figure 7. Using this method, the stress spectrum is treated, in a simplified way, as a set of n load blocks with the constant stress range $\Delta\sigma = \sigma_{max} - \sigma_{min}$.

The resistance to fatigue is mathematically estimated by means of accumulation of individual damage caused by individual stress blocks of each stress set. The number of stress sets is defined by the number of analysed frequency modes and the number of critical positions in which the vortex separation occurs.

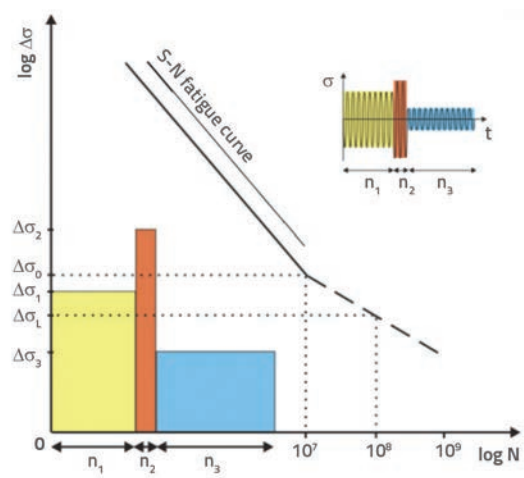

Figure 7. Calculation principle using cumulative damage method

Proving fatigue resistance according to the theory of cumulative damage is generally a highly complex task for the engineering practice. The set of stress ranges is required for successful fatigue check, i.e. for defining the sum of damage. However, the number of stress-ranges due to vortex shedding is limited , and computation according to this method is not overly demanding in the case of vortex shedding. A possible alternative to this approach is the use of the concept of equivalent damage factors. For this computation approach, defined in EN 1993-1-9 [40], the equivalent stress range $\Delta\sigma_{E,2}$ can be defined according to:

$$\gamma_{Ff} \cdot \Delta\sigma_{E,2} = \lambda \cdot \Delta\sigma(\gamma_{Ff} \cdot Q_k) \qquad (30)$$

where :

- γ_{Ff} - partial factor for actions, i.e for the equivalent constant stress ranges
- $\Delta\sigma_{E,2}$ - equivalent constant amplitude stress range for 2 million cycles
- Q_k - characteristic value of a single variable action.

Proof of resistance to fatigue can be expressed as follows (31):

$$\gamma_{Ff} \cdot \Delta\sigma_{E,2} \leq \Delta\sigma_c / \gamma_{Mf} \qquad (31)$$

where:

- $\Delta\sigma_c$ - reference value of fatigue strength at 2 million cycles
- γ_{Mf} - partial factor for fatigue strength.

The equivalent damage factor is specified for individual types of structures in appropriate parts of Eurocode EN 1993. In case of vertical load-bearing elements presented in this paper, it is appropriate to use the equivalent damage factor according to EN 1993-3-1 [41] and EN 1993-3-2 [42]. For an arbitrary spectrum, an equivalent stress range corresponding to 2 million oscillation cycles can be determined according to Eurocode, but with some restrictions. In fact, material fatigue curves from EN 1993-1-9 define double slope, m = 3 or m = 5. As only one slope of the S-N curve is defined in [41] by expression (9.3), there is a limitation that cannot be avoided without adopting assumptions that are not covered by the standard. In a general case, for one-sided slope of the S-N curve, according to expression (9.3) from [41], the reference stress range for the selected reference number of cycles can be written as follows (32):

$$\Delta\sigma_{E,ref} = \left(\sum_i \frac{n_i \Delta\sigma_i^m}{N_{ref}} \right)^{\frac{1}{m}} \qquad (32)$$

where:

- $\Delta\sigma_{E,ref}$ - reference stress range for the selected reference number of cycles N_{ref}
- n_i - number of stress cycles in spectrum block i
- $\Delta\sigma_i$ - stress range in spectrum block i
- m - slope of the fatigue curve, i.e. stress exponent of the fatigue curve.

The method of equivalent damage factors with the constant equivalent stress range is widely used in the case of steel structures of cylindrical type, such as steel chimneys. These structures are characterized by oscillation in fundamental mode, and so this mode is normally taken into account when determining fatigue of material. Here it is possible to determine the equivalent damage factor, i.e. the equivalent stress range without much complications by means of (9.3) from [41] or (32). On the other hand, the oscillation in second mode is typical for tapered structures, and so this method would prove to be overly complex and, in the authors' opinion, inadequate for everyday use, as it requires adoption of computation principles that are not defined by Eurocode. This method will therefore not be used in the computation example presented in this paper.

It should be noted that Eurocode defines the value of partial coefficient for verifying resistance to fatigue γ_{Mf} as ranging from 1.0 to 1.35 depending on damage-tolerant and safe-life criteria, and consequences of possible failure. It is not unusual to use the value of 1.0 for this parameter in the case of structures for which regular maintenance and checking of connection details is obligatory. However, as structures subjected to vortex shedding are typically situated in urban areas, it may reasonably be stated that their failure would represent an imminent danger for the surrounding area. In such cases, according to the authors' opinion, and based on the damage-tolerant and safe-life concept, it is necessary to adopt at least the partial coefficient γ_{Mf} = 1.15 for significant consequences in case of failure. Based on the aforementioned theory, the nominal stress calculated in closed form for cross-section requiring calculation of resistance to fatigue can be presented in the following form (33):

$$\sigma_{ij,max}(t) = \frac{M_{ij}(t)}{W_{ij}} \qquad (33)$$

where W_{ij} is the moment of resistance of critical cross-section, and $M_{ij}(t)$ can be calculated using the mentioned calculation procedure based on the finite element method according to expression (17), or based on time integration in resonant area, i.e. using modal analysis (Figure 6). Calculated stresses constitute nominal stresses, based on net area of cross-section of the basic material. Although classification of calculation approaches for estimating fatigue of material is not the subject of this paper, it should be noted that the method of nominal stresses is a conservative global approach that requires the least amount of time. Figure 8 shows calculation approaches that are most often used in current practice. It can be noted that the accuracy of results obtained using the nominal stress method decreases with an increase in complexity of the detail that is being analysed. In addition, the S-N curve for a particular detail is often not available in practical situations, which additionally complicates the calculation. In such cases, the use of the hot-spot-stress method is obligatory. This is only very superficially treated in [40] and so it is often necessary to use additional literature sources, primarily IIW recommendations [43] and

DNV recommended practice [44], especially with regard to the rules considering adoption of the size and type of final elements and the stress extrapolation rules. The ENS-Method (Effective Notch Stress Method) is an even more comprehensive method, and the most complex procedure involves the use of LEFM (Linear Elastic Fracture Mechanics) approach.

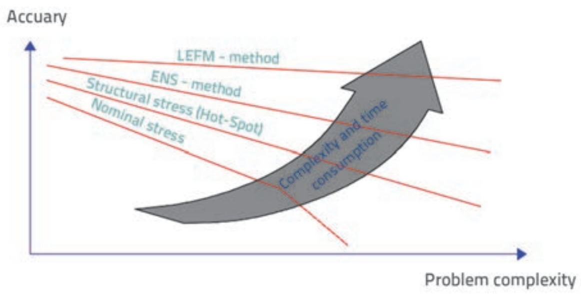

Figure 8. Comparison of the most frequently used fatigue analysis methods

3.3. Assessment of number of stress cycles and lock-in phenomenon

The theory presented by Repetto and Solari can also be used for the calculated nominal stresses. These authors offered a closed solution for fatigue analysis due to oscillation of slender cantilever beams parallel and perpendicular to the direction of wind [45-47]. The approach presented in [45, 47] can in principle be adopted, with additional generalisation based on assumptions of the vortex-resonance model and according to [48]:

- the resonance method assumes harmonic response of the system in lock-in state;
- for all reference critical velocities entering in the range of resonant frequency, the calculated resonance response is considered to be the maximum value in this critical range, $\Delta\sigma = \sigma_{max} - \sigma_{min} = 2\sigma_{max}$.

As a consequence of these assumptions, the defined stress amplitude probability can be treated as unique, $P(\Delta\sigma_n)$, which is why the total number of structural oscillations in the i-th mode of oscillation $n_i(\Delta\sigma_{ir})$ (34) during the time interval T expressed in years, amounts to:

$$n_i\left(\Delta\sigma_i\right) = n_{i,y} \cdot T \cdot P_U(U_i^*) \tag{34}$$

where $P_U(U_i^*)$ defines the probability of occurrence of critical velocity that can cause resonant state in critical cross-section at the height $z = z^*$, in mode i. When wind direction is taken into account, i.e. when there is a significant variation in local roughness of terrain in a particular direction, the number of structural oscillations $n_i(\Delta\sigma_{ir})$ (34) becomes:

$$n_{ir}\left(\Delta\sigma_{ir}\right) = n_{i,y} \cdot T \cdot P_U(U_{ir}^*) \cdot \mathrm{P}_\theta(\theta_{ir}) \tag{35}$$

where $P_\theta(\theta_{ir})$ defines the probability of occurrence of the mean critical velocity of wind in the direction r.

It remains unclear what limits of the critical wind velocity should be adopted in the analysis. It has already been stated that the deviation of wind velocity that exceeds the one causing lock-in is not included in empirical parameter of the effective correlation length, and this fact has to be taken into account during estimation of the number of oscillations the structure is subjected to during excitation. The range of critical velocity limits has been extensively studied by professional community. Two limit cases can be observed. Ruscheweyh [13, 30] states that non-symmetry of the frequency range can be noted, which was used by Clobes et al. [49] when defining eccentricity of 2/5 as related to 3/5 of the total resonance area. An alternative approach was proposed by Simiu and Scanian (summarized in [50]), where the reference critical velocity is defined as the lower limit of critical area, $u_{crit,low} = v_{crit}$, with maximum bandwidth of ≈ 0.30 ($u_{crit,high} \approx 1.30 u_{crit,low}$).

The mean value of bandwidth of $\varepsilon_0 = 0.20$ is adopted in this paper according to [1], with definition of the already mentioned eccentricity according to [49], (Figure 9). Results are calculated for the statistical model based on the Weibull distribution with the shape and scale parameters adopted for the location at which the structure is situated. The comparison is made with the proof of material fatigue that is calculated based on the number of cycles according to EN 1991-1-4 (E.10) [1], for the standard function of density distribution with the shape and scale factors of k = 2 and $u_0 = 1/5\ u_{m,Lj}$, where $u_{m,Lj}$ is the reference mean velocity of wind at the height of critical cross-section at which the vortex is formed.

Future research can be oriented towards application of numerical methods based on CFD (computational fluid dynamics), as in [51], and towards experimental research, as in [52]. These approaches enable study of application of the system for reducing resonant oscillation, such as TMD (Tuned Mass Damper) systems or spiral aerodynamic dampers (helical strakes). It should be noted that transition zone at the occurrence of lock-in still constitutes an unexplored area. That is why the authors plan to use CFD programs to undertake new research of the influence of lock-in on the occurrence of additional harmonic components that amplify the oscillation amplitude.

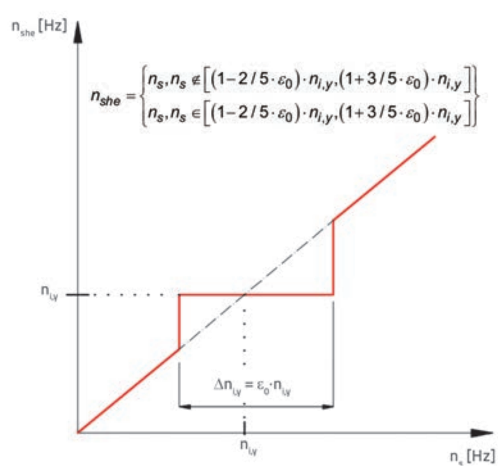

Figure 9. Lock-in model

4. Numerical example

A steel pole for stadium lighting, of variable cross-section, 37.9 m in height, is considered.

The objective is to calculate, using the previously defined calculation procedure, the pole structure oscillation amplitude due to vortex shedding, and to provide the check of material fatigue for the critical details using the Palmgren-Miner theory of cumulative damage.

As to the mean wind velocity profile, design parameters correspond to the wind zone 2, and terrain category II-III, according to [1, 26]. It is assumed that the structure is located in Hannover (52°27'00''N 09°42'00''E), with the mean coefficients of Weibull distribution amounting to A = 4.50, k = 1.79, according to [53], Figure 10. At the top, the structure measures 500 mm in diameter, the slope of the structure is 25 mm/m, and the wall length and thickness of 16-angle cross-sections amount to: 9700 mm/5 mm; 1200 mm/6 mm, 1200 mm/8 mm, 9300 mm/12,5 mm – measuring from top to bottom.

It is assumed that the critical position of vortex shedding is at antinode points, i.e. at the positions of local amplitudes of oscillation modes, although it can be seen in Figure 11 that the vortex separation at these cross-sections is not likely due to the effect of aerodynamic disturbance of fluid flow by the platform and the supporting structure of floodlights for stadium lighting. Frequency characteristics of the structure were tested for the case of 1D and 3D structure, and less favourable calculation results were finally adopted as relevant, cf. Figure 11. Nodal masses shown in Figure 11 are presented in tabular form for clarity reasons.

Calculation parameters adopted in the analysis are given in Table 2. Calculated values for vortex shedding in the first two oscillation modes for H_{crit} = 36.36 m and H_{crit} = 21.73 m are given in Table 3, while the bending moment values for cross-sections in which fatigue resistance is checked are given in Table 4.

Figure 10. Weibull distribution according to [53] – for measuring instrument placed at the height of 10 m, Hannover

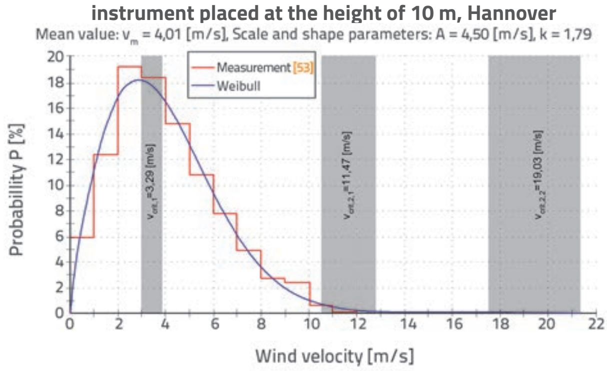

Connection details for which the fatigue check was made are shown in Figure 12. The category 80 according to Table 8.4 [40] was adopted for the cross-section at the bottom of the pole (Figure 12, bottom). In this case, the critical detail under consideration is the fillet weld at the connection between the annular horizontal compression ring and the steel pole. The detail at the top part of Figure 12 is the longitudinal automatic weld that has to be checked for fatigue at the point of slip-joint used for the extension of the structure, where local stiffness change occurs due to the overlap of steel shell elements with the variable thickness. The category 140 was adopted for this extension, Figure 12. Control checks of other details will not be shown in order to simplify the numerical example. It can be noted that bending moment at the bottom of the pole has

Table 2. Computation parameters

$n_{i,y}$ [Hz]	m_e [kg/m]	St [-]	δ_s [-]	ρ [kg/m^3]	ν [m^2/s]
1.095	170.213	0.18	0.015	1.250	1.5 10^{-5}
3.821	230.468	0.18	0.015	1.250	1.5 10^{-5}

Table 3. Calculated values for vortex shedding in first two oscillation modes

$n_{i,y}$ [Hz]	H_{crit} [m]	v_{crit} [m/s]	c_{lat} [-]	Sc [-]	Re [-]	K [-]	K_w [-]	$y_{F,max}$ [mm]
1.095	36.36	3.29	0.700	13.98	118477	0.131	0.245	26.8
3.821	36.36	11.47	0.386	18.93	413491	0.184	0.463	28.9
3.821	21.73	19.03	0.200	6.89	1136788	0.184	0.463	68.3

Table 4. Bending moments [kNm]

$n_{i,y}$ [Hz]	z = 0 [m]	z = 9.3 [m]	z = 19.2 [m]	z = 29.5 [m]
1.095	78.0	50.8	23.8	5.6
3.821	272.6	75.5	73.1	54.5
3.821	643.9	178.3	172.8	128.8

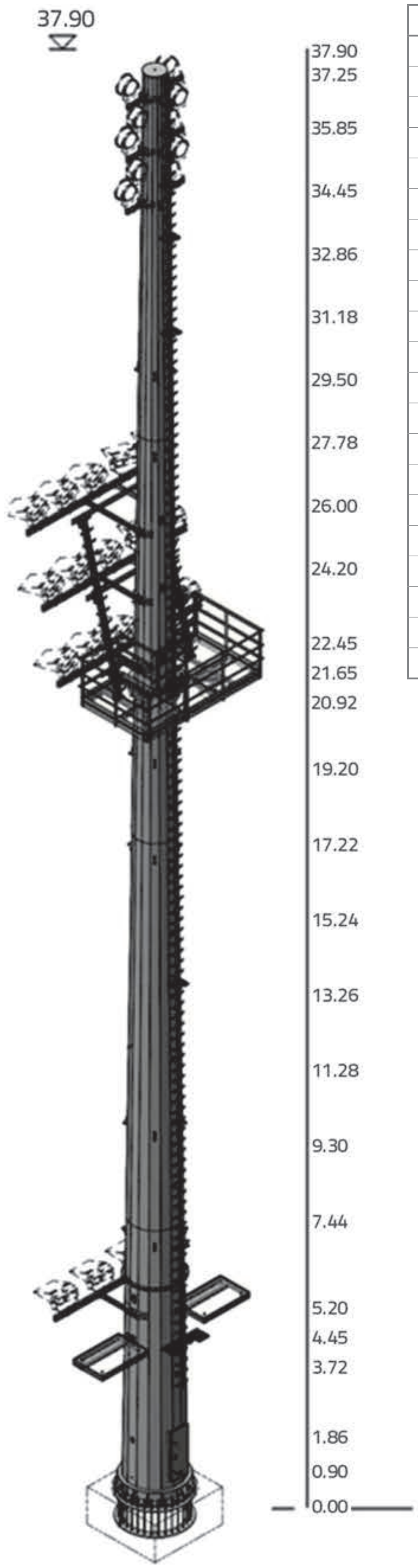

Nr [-]	z [m]	m [kg]	Nr [-]	z [m]	m [kg]
41	37.90	46.66	20	21.70	807.49
40	37.30	123.98	19	21.65	109.80
39	37.25	82.85	18	20.92	265.08
38	35.22	26.43	17	19.20	247.89
37	35.90	114.20	16	19.20	410.50
36	35.85	111.68	15	17.22	430.09
35	34.54	67.92	14	15.24	449.68
34	34.45	143.20	13	13.26	469.27
33	32.86	159.93	12	11.28	488.85
32	31.18	168.74	11	9.30	508.38
31	29.50	117.12	10	9.30	717.82
30	29.50	209.86	9	7.44	744.83
29	27.78	220.90	8	5.58	134.97
28	26.07	308.87	7	5.25	220.73
27	26.00	223.08	6	5.20	289.18
26	24.35	13.85	5	4.50	241.02
25	24.25	287.01	4	4.45	305.94
24	24.20	222.13	3	3.72	798.85
23	22.63	19.33	2	1.86	422.88
22	22.50	267.34	1	0.90	389.48
21	22.45	110.07	0	0.00	264.54

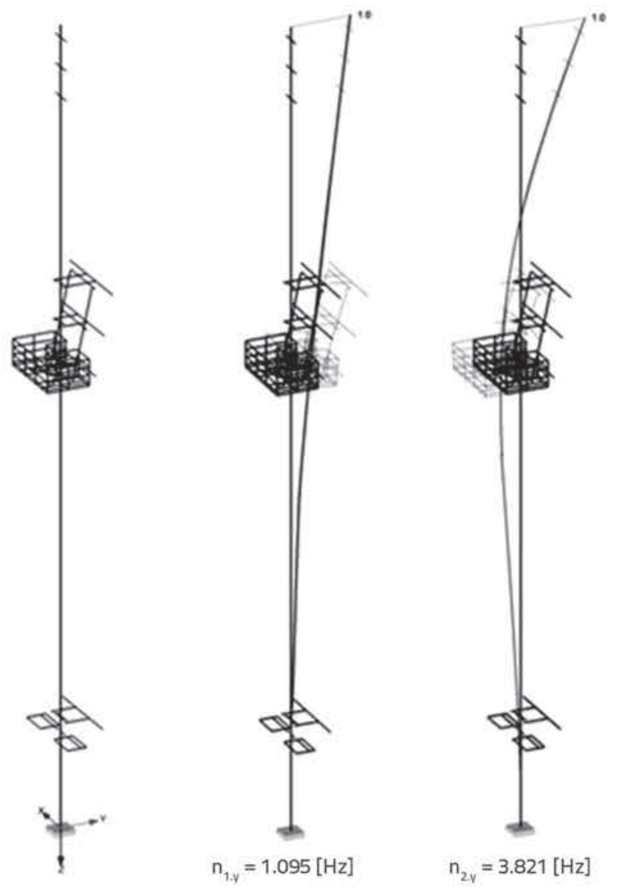

Figure 11. 3D-CAD Model of the structure, nodal mass distribution for 1D structure and oscillation modes for 3D girder

the maximum oscillation value in the second mode for vortex shedding at the height of 21.73 m – Table 4.

The maximum oscillation amplitude of 68.3 mm is also obtained at oscillation in the second mode with vortex shedding at the height of 21.73 m – Table 3. The dimensionless amplitude $y_{F,max}/b$ amounts to 0.076 and so there is no need for iterative increase of effective correlation lengths which, in the second mode, amount to: L_1 = 3.24 m and L_2 = 5.38 m.

Table 5. Result of fatigue analysis for cross-sections at various heights using cumulative damage concept, for Weibull wind distribution according to [53]

z = 29.50 [m]. γ_{Mf} = 1.15. γ_{Ff} = 1.00. $\Delta\sigma_c$ = 140 [N/mm²]			
	A = 4.50. *k* = 1.79. according to [53]		
	First oscillation mode	Second oscillation mode, H_{crit} = 36.36 m	Second oscillation mode, H_{crit} = 21.73 m
$\Delta\sigma$	5.69	55.90	132.07
n	1.98×10^8	5.19×10^7	6.82×10^4
N	Infinite	5.32×10^7	5.32×10^6
D	0.000	0.976	0.013
z = 19.20 [m]. γ_{Mf} = 1.15. γ_{Ff} = 1.00. $\Delta\sigma_c$ = 140 [N/mm²]			
	A = 4.50. *k* = 1.79. according to [53]		
	First oscillation mode	Second oscillation mode, H_{crit} = 36.36 m	Second oscillation mode, H_{crit} = 21.73 m
$\Delta\sigma$	11.2	34.30	80.97
n	1.98×10^8	5.19×10^7	6.82×10^4
N	Infinite	Infinite	8.34×10^6
D	0.000	0.000	0.008
z = 9.30 [m]. γ_{Mf} = 1.15. γ_{Ff} = 1.00. $\Delta\sigma_c$ = 140 [N/mm²]			
	A = 4.50. *k* = 1.79. according to [53]		
	First oscillation mode	Second oscillation mode, H_{crit} = 36.36 m	Second oscillation mode, H_{crit} = 21.73 m
$\Delta\sigma$	11.50	17.10	40.41
n	1.98×10^8	5.19×10^7	6.82×10^4
N	Infinite	Infinite	Infinite
D	0.000	0.000	0.000
z = 0.00 [m]. γ_{Mf} = 1.15. γ_{Ff} = 1.00. $\Delta\sigma_c$ = 80 [N/mm²]			
	A = 4.50. *k* = 1.79. according to [53]		
	First oscillation mode	Second oscillation mode, H_{crit} = 36.36 m	Second oscillation mode, H_{crit} = 21.73 m
$\Delta\sigma$	8.20	28.50	67.37
n	1.98×10^8	5.19×10^7	6.82×10^4
N	Infinite	9.38×10^7	2.20×10^6
D	0.000	0.553	0.031

Fatigue analysis results based on expression (29), for statistical data according to Weibull distribution as per [53], are presented in tables 5 and 6.

Table 6. Results of fatigue analysisfor cross-sections at various heights using cumulative damage concept, for Weibull distribution according to [53] - total damage

Figure 12. Connection detail with selected categories and Wöhler-lines (S-N fatigue curves)

z [m]	ΣD [-]
29.5	0.989
19.22	0.008
9.3	0.000
0	0.584

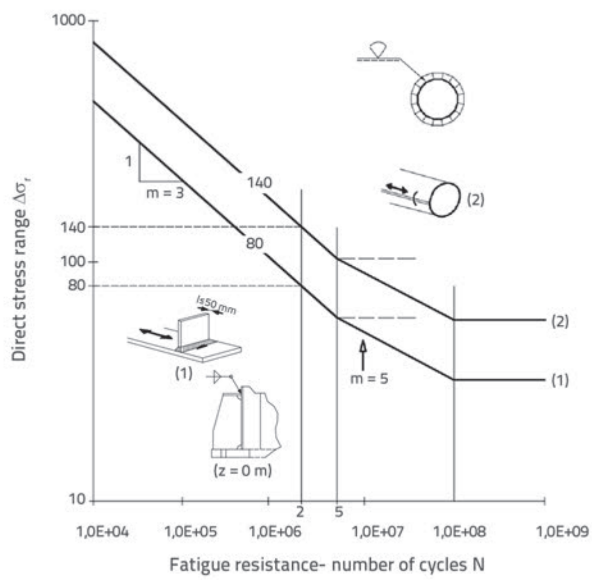

The analysis of calculated values presented in Table 6 shows that the structure is safe and that the fatigue resistance check based on the cumulative damage theory predicts no damage occurrence during the 50 years of lifetime for the mean wind profile according to Weibull distribution, adopted according to [53]. For comparison, the fatigue resistance check was also provided for the number of load cycles defined according to (E.10) [1], with the factors of shape and scale amounting to $k = 2$ and $u_0 = 1/5\ u_{m,Lj}$, where $u_{m,Lj}$ is the reference mean wind velocity at the height of critical cross-section in which vortex separation occurs. Results are presented in tables 7 and 8.

The analysis of values presented in Table 8 indicates that the structure is not safe and that the fatigue resistance check based on the Palmgren-Miner theory predicts the damage occurrence during the 50-year design lifetime of the structure. There is a big difference in calculated cumulative damage when results from Table 6 are compared with those from Table 8 for the cross section at the height of 29.5m and for the cross section at the bottom of the pole. The difference in calculated damage can be described with factor 4.10 for the detail at the height of 29.5 m, and with factor 3.95 for the detail at the bottom of the pole.

Table 7. Result of fatigue analysis for cross-sections at various heights using cumulative damage concept, for the assumed number of cycles according to (E.10) [1], k = 2, $v_0 = v_{m,Lj}/5$

z [m]	ΣD [-]
29.5	4.057
19.22	0.006
9.3	0.000
0	2.307

Table 8. Results of fatigue analysis for cross-sections at various height using cumulative damage concept, for assessment of the number of cycles according to (E.10) [1], k = 2, $v_0 = v_{m,Lj}/5$

z = 29.50 [m]. γ_{Mf} = 1.15. γ_{Ff} = 1.00. $\Delta\sigma_c$ = 140 [N/mm²]			
	EN 1991-1-4 . k = 2. $v_0 = v_{m.Lj}/5$. ε_0 = 0.20		
	First oscillation mode	Second oscillation mode, H_{crit} = 36.36 m	Second oscillation mode, H_{crit} = 21.73 m
$\Delta\sigma$	5.69	55.90	132.07
n	1.56×10^8	2.14×10^8	5.34×10^4
N	Infinite	5.32×10^7	1.57×10^6
D	0.000	4.023	0.034
z = 19.20 [m]. γ_{Mf} = 1.15. γ_{Ff} = 1.00. $\Delta\sigma_c$ = 140 [N/mm²]			
	EN 1991-1-4 . k = 2. $v_0 = v_{m.Lj}/5$. ε_0 = 0.20		
	First oscillation mode	Second oscillation mode, H_{crit} = 36.36 m	Second oscillation mode, H_{crit} = 21.73 m
$\Delta\sigma$	11.2	34.30	80.97
n	1.56×10^8	2.14×10^8	5.34×10^4
N	Infinite	Infinite	8.34×10^6
D	0.000	0.000	0.006
z = 9.30 [m]. γ_{Mf} = 1.15. γ_{Ff} = 1.00. $\Delta\sigma_c$ = 140 [N/mm²]			
	EN 1991-1-4 . k = 2. $v_0 = v_{m.Lj}/5$. ε_0 = 0.20		
	First oscillation mode	Second oscillation mode, H_{crit} = 36.36 m	Second oscillation mode, H_{crit} = 21.73 m
$\Delta\sigma$	11.50	17.10	40.41
n	1.56×10^8	2.14×10^8	5.34×10^4
N	Infinite	Infinite	Infinite
D	0.000	0.000	0.000
z = 0.00 [m]. γ_{Mf} = 1.15. γ_{Ff} = 1.00. $\Delta\sigma_c$ = 80 [N/mm²]			
	EN 1991-1-4 . k = 2. $v_0 = v_{m.Lj}/5$. ε_0 = 0.20		
	First oscillation mode	Second oscillation mode, H_{crit} = 36.36 m	Second oscillation mode, H_{crit} = 21.73 m
	8.20	28.50	67.37
n	1.56×10^8	2.14×10^8	5.34×10^4
N	Infinite	9.38×10^7	2.20×10^6
D	0.000	2.281	0.026

Displacements over time of the point at the top of the structure at vortex shedding in critical cross-section at the heights of H_{crit} = 36.36 m and H_{crit} = 21.73 m for the case of resonant oscillation in the first and second modes, respectively, are shown in Figure 13. Sensitivity to vortex-resonance of the structure is greater for oscillation in the second mode where the oscillation amplitude attains approximately 7 seconds after the application of harmonic forces (20). This information in combination with the calculated Scruton number amounting to 6.89 (Table 3) leads to the conclusion that this is a border case, and that further increase in pole slenderness or optimisation by mass or stiffness reduction would potentially lead to significant resonance problems.

Figure 13. Displacements of y_F point at the top of the structure over time t, for α = 0.00376, β = 0.00123

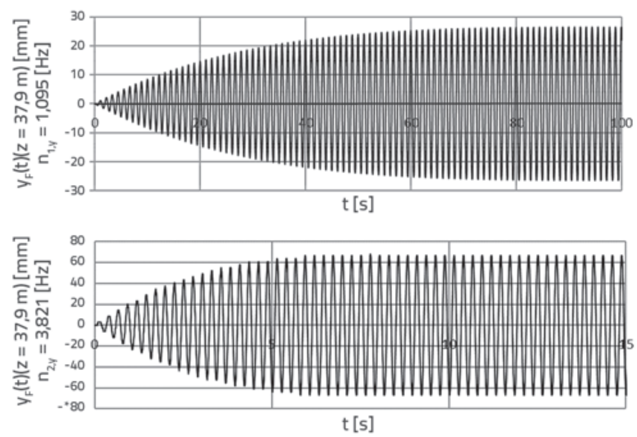

5. Conclusion

Free-standing structures are often subjected to cyclic vortex oscillations. Actions from vortex shedding can be determined by means of appropriate computation methods and adequate verifications can be made at critical points along the structure. The calculation procedure for determining resistance of material to fatigue due to vortex shedding is presented in this paper, by assessing fatigue using the Palmgren-Miner method of cumulative damage.

It is shown in the text in which way the wind profile influences the prediction of the number of loading cycles and, finally, how the same influences the total accumulated damage. The authors' experience shows that the results of cumulative damage assessment do not always need to be more favourable and economical when wind profile is used at the location where the structure is realized. Based on the use of the calculation procedure presented in this paper on more than 1000 concrete and hybrid telecommunication poles, the authors have established that, with regard to estimation of amplitude and number of loading cycles, the Eurocode model shows adequate results during calculation of structures situated in Central European countries. A considerable inconsistency has been noted in assessment during design of steel structures in Northern Europe, in littoral areas, and in zones with small local roughness of terrain and laminar wind, such as airport zones. This points to the need for undertaking additional research of this phenomenon, which has to be transferred from the calculation aspect to the experimental area, involving observation of response of existing structure in order to correct computation models.

A proper calculation approach is possible only by using a specialized program that implements the presented theory. The presented calculation approach based on vortex resonance model from EN 1991-1-4 takes appropriately into account all significant parameters that bear influence on the estimation of results.

Inconsistencies and unknowns in the use of Eurocode, as related to the selection of parameters and computation methods, are presented in the paper. A special emphasis is given to the significance of the presented iterative calculation procedure in case of structures in which geometrical conditions deviate from assumptions of the vortex-resonance model. In such cases, the effects of aeroelastic forces must be appropriately introduced in the analysis, by increasing the effective correlation length.

As the total damage is also influenced by oscillation in the wind direction, future research work should also concentrate on the analysis of influences during such oscillation of structures.

REFERENCES

[1] EN 1991-1-4:2005 - Eurocode 1. Action on structures. General actions. Wind actions.

[2] Model Code for Steel Chimneys - the CICIND Chimney Standard, ISBN 1-902998-16-2, Revision 2010, Zürich, Switzerland.

[3] NRCC 48192, National Research Council Canada, User´s Gudie-NBC 2005 Structural Commentaries (Part 4 of Division B), ISBN 0-660-19506-2, 1993.

[4] DS410 E:2004, Code of Practice for Loads for the Design of Structures, Danish Standard Association, 2004.

[5] AS/NZS 1170.2:2002, Australian/New Zealand Standard, Structural design actions, Part 2: Wind Actions, 2005.

[6] ESDU 96030. 1996. Response of structures to vortex shedding: Structures of circular or polygonal cross-section. Engineering Sciences Data Unit (ESDU International, London, UK), ESDU Data Item 96030.

[7] ESDU 96031- Computer programs for response of structures to vortex shedding. Structures of circular or polygonal cross section. Part 1. Microsoft Excel module, Engineering Sciences Data Unit (ESDU International, London, UK), ESDU Data Item 96031.

[8] Holmes, D.J.: Wind Loading of Structures, 3rd Edition, CRC Press, 2014.

[9] Ruscheweyh, H.: Vergleich der zwei Berechnungsverfahren für Querschwingungen, Deutsches Ingenieurblatt - Forschung + Technik, DIB 4, 2015.

[10] Clobes, M., Willecke, A., Peil, U.: Wirbelerregung von Stahlschornsteinen-zwei Grenzzustände der Tragfähigkeit und Vorschlag für die Bemessung, FT Windtechnologie, Band 87, Mai 2012.

[11] Dyrbye, C., Hansen, O.S.: Wind Loads on Structures, Wiley, January 1997.

[12] Hansen, S.O.: Vortex-induced vibrations of structures, Structural Engineers World Congress 2007, November 2-7, 2007. Bangalore, India.

[13] Ruscheweyh, H.: Ein verfeinertes praxisnahes Berechnungsverfahren wirbelerregter Schwingungen von schlanken Baukonstruktionen im Wind, Aufl. Inst. für Mech., Heft 20, 1987.

[14] Ruscheweyh, H.: Practical experiences with wind-induced vibrations, Journal of Wind Engineering and Industrial Aerodynamics, 33 (1990), pp. 211-218.

[15] Ruscheweyh, H., Sedlacek, G.: Cross-wind vibrations of steel stacks - Critical comparisons between some recently proposed codes, Journal of Wind Engineering and Industrial Aerodynamics, 33 (1988), pp. 173-183.

[16] Galemann, T., Ruscheweyh, H.: Untersuchung winderregter Schwingungen an Stahlschornsteinen. Forschungsbericht Projekt 163 - Lehrstuhl für Stahlbau, RWTH Aachen, 1992.

[17] Galemann, T., Ruscheweyh, H.: Untersuchung Winderregter Schwingungen an Stahlschornsteinen - Stahlschornsteinbau fortschlictliche Lösungen, Essen : Vulkan - Verlag, 1992.

[18] Ruscheweyh, H.: Interferenzwirkung zwischen Schornstein und Gebäude auf die wirbelerregte Schwingung; WTG-Mitt, Nr. 5, Baukonstruktion unter Windeinwirkung, 1992.

[19] Niemann, H.J., et. all: Vibrations of Chimneys under the Action of the Wind - Proceedings of the 9th International Conference on Structural Dynamics, EURODYN 2014 Porto, Portugal, 30 June - 2 July 2014 A. Cunha, E. Caetano, P. Ribeiro, G. Müller (eds.) ISSN: 2311-9020; ISBN: 978-972-752-165-4.

[20] Holmes, J.D.: Response of cylindrical structures to vortex shedding in the natural wind - 13th Australian Fluid Mechanics Conference Monash University, Melbourne, Australia, 13-18 December 1998.

[21] Verboom, V.K., van Koten, H.: Vortex excitation: Three design rules tested on 13 industrial chimneys - Journal of Wind Engineering and Industrial Aerodynamics, 98 (2010), pp. 145-154.

[22] Vickery, B.J., Clark, A.W.: Lift or across-wind response of tapered stacks, Journal of Structural Division, ASCE, 98 (1972), pp. 1-20.

[23] Vickery, B.J., Basu, R.I.: Across-wind vibrations of structures of circular cross-section. Part I - Development of a mathematical model for two-dimensional conditions. Journal of Wind Engineering and Industrial Aerodynamics, 12 (1983), pp. 49-73.

[24] Vickery, B.J., Basu, R.I.: Across-wind vibrations of structures of circular cross-section. Part II - Development of a mathematical model for full-scale application. Journal of Wind Engineering and Industrial Aerodynamics, 12 (1983), pp. 75-97.

[25] Vickery, B.J., Basu, R.I.: The response of reinforced concrete chimneys to vortex shedding. - Engineering structures, 6 (1984), pp. 324-333.

[26] DIN EN 1991-1-4/NA:2010-12 - Nationaler Anhang - National festgelegte Parameter - Eurocode 1: Einwirkungen auf Tragwerke - Teil 1-4: Allgemeine Einwirkungen - Windlasten

[27] NF EN 1991-1-4/NA:2005 - Eurocode 1 : Actions sur les structures — Partie 1-4 : Actions générales — Actions du vent Annexe nationale à la NF EN 1991-1-4, Actions générales — Actions du vent

[28] Scruton, C.: An Introduction to Wind Effects on Structures - Oxford University Press, Oxford, UK, 1981

[29] Rumman, W.S.: Basic structural design of concrete chimneys. ASCE, Journal of the Power Division, 96 (1970), pp. 309-318.

[30] Ruscheweyh, H.: Dynamische Windwirkung an Bauwerken, Band 2 - Praktische Anwendungen. Bauverlag GmbH, Wiesbaden und Berlin,1982

[31] Dickel, T., Rothert, H.: Anmerkungen und computerorientierte Berechnungshilfen zum Querschwingungsnachweis nach DIN 4131 und DIN 4133, Bauingenieur, 69 (1994), pp. 403-408.

[32] Verwiebe, C.: Fatigue Problems of Steel Chimneys due to Vortex Excited Vibrations in the Second Mode - IDN - CICIND REPORT, 20 (2004) 2.

[33] Guide for the assessment of wind actions and effects on structures, National Research Council of Italy, June 2010.

[34] Dickel, T., Rothert, H.: Berechnungshilfen für einfache Fälle des Querschwingungsnachweises nach DIN 4131 und DIN 4133, Bauingenieur, 69 (1994), pp. 239-246.

[35] Dickel, T.: PC-Programm EASYKAM: Nachweis der Querschwingungen DIN 4133/4131, Schwabach 1988.

[36] Dickel, T.: Zur Verwendung von Eigenformen in DIN 4131 und DIN 4149, Tipp des Monats 10/04, Prüfamt für Baustatik, Nürnberg, 2004.

[37] Novak, M., Tanaka, H.: Pressure Correlations On a Vibrating Cylinder. Proc. 4th International Conference Wind Effects on Building and Structures, London 1975. Cambrige: University Press 1977.

[38] https://www.dlubal.com/de/produkte/rfem-und-rstab-zusatzmodule/sonstige/rf-com, pristupljeno 21.01.2018.

[39] Ruscheweyh, H.: Windlastannahmen für turmartige Bauwerke. In: Referatensammlung. Türme, Maste, Schornsteine in Stahl. Fürth, pp. 3-1 do 3-20, Berlin, Köln: Beuth 1992.

[40] EN 1993-1-9:2005 - Eurocode 3: Design of steel structures - Part 1-9: Fatigue.

[41] EN 1993-3-1: 2009 - Eurocode 3: Design of steel structures - Part 3:1 - Towers, masts and chimneys - Towers and masts.

[42] EN 1993-3-2: 2009 - Eurocode 3: Design of steel structures - Part 3:1 - Towers, masts and chimneys - Chimneys.

[43] IIW Document IIW-1823-07, ex XIII-2151r4-07/XV-1254r4-07: Recommendations for fatigue design of welded joints and components - International Institute of Welding, December 2008.

[44] DNV-GL Recommended Practice - Fatigue design of offshore steel structures; DET-Norske-Veritas AS Germanischer Lloyd SE (DNV GL AS), April 2016;.

[45] Repetto, M.P., Solari, G.: Dynamic along-wind fatigue of slender vertical structures, Engineering Structures, 23 (2001) 12, pp. 1622-1633.

[46] Repetto, M.P., Solari, G.: Diagnosis of Fatigue Collapses of Slender Structures due to Aerodynamic Wind Actions; BBAA VI International Colloquium on: Bluff Bodies Aerodynamics & Applications, Milano, Italy, 2008.

[47] Repetto, M.P., Solari, G.: Crosswind Response Induced Fatigue of Slender Structues, 8th ASCE Specialty Conference on Probabilistic Mechanics and Structural Reliability, University of Notre Dame, Indiana, 2000.

[48] Pasto, S.: Fatigue-Induced Risk Assessment of Slender Structures with Circular Cross-Section at Lock-In; Dissertation, Department of Civil Engineering of the TU Carolo-Wilhelmina at Braunschweig, 2005.

[49] Clobes, M., Willecke, A., Peil, U.: Vortex-induced vibrations of slender structures considering long-term wind profile statistics, Proceedings of the 8th International Conference on Structural Dynamics, EURODYN 2011 Leuven, Belgium, 4-6 July 2011, ISBN 978-90-760-1931-4.

[50] Simiu, E., Scanlan, R.H.: Wind effects on structures. Wiley, New York, 1986.

[51] Vegard, H., Tahsin, T., Elif, O.: Full-scale CFD investigations of helical strakes as a means of reducing the vortex induced forces on a semi-submersible, Ocean Engineering, 137 (2017) C, pp. 338-351, https://doi.org/10.1016/j.oceaneng.2017.04.014

[52] Juan, S., Jiasong, W., Shengping, L., Qilong, T.: VIV suppression for a large mass-damping cylinder attached with helical strakes, Journal of Fluids and Structures, 62 (2016) C, pp. 125-146, https://doi.org/10.1016/j.jfluidstructs.2016.01.005

[53] Troen, I., Lundtang Petersen, E.: European Wind Atlas. Roskilde: Risø National Laboratory, Denmark, 1989.